J. Am. Soc. Mass Spectrom. (2014) 25:1572–1582
DOI: 10.1007/s13361-014-0936-6

RESEARCH ARTICLE

Determination of Internal Energy Distributions of Laser Electrospray Mass Spectrometry using Thermometer Ions and Other Biomolecules

Paul M. Flanigan IV,[1,2] Fengjian Shi,[1,2] Johnny J. Perez,[1,2] Santosh Karki,[1,2] Conrad Pfeiffer,[1] Christian Schafmeister,[1] Robert J. Levis[1,2]

[1]Department of Chemistry, Temple University, Philadelphia, PA 19122, USA
[2]Center for Advanced Photonics Research, Temple University, Philadelphia, PA 19122, USA

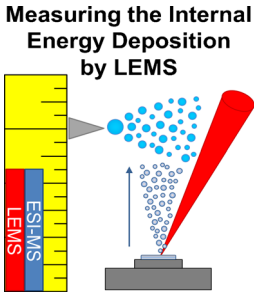

Abstract. The internal energy distributions for dried and liquid samples that were vaporized with femtosecond duration laser pulses centered at 800 nm and postionized by electrospray ionization-mass spectrometry (LEMS) were measured and compared with conventional electrospray ionization mass spectrometry (ESI-MS). The internal energies of the mass spectral techniques were determined by plotting the ratio of the intact parent molecular features to all integrated ion intensities of the fragments as a function of collisional energy using benzylpyridinium salts and peptides. Measurements of dried p-substituted benzylpyridinium salts using LEMS resulted in a greater extent of fragmentation in addition to the benzyl cation. The mean relative internal energies, $<E_{int}>$ were determined to be 1.62±0.06, 2.0±0.5, and 1.6±0.3 eV for ESI-MS, dried LEMS, and liquid LEMS studies, respectively. Two-photon resonances with the laser pulses likely caused lower survival yields in LEMS analyses of dried samples but not liquid samples. In studies with larger biomolecules, LEMS analyses of dried samples from glass showed a decrease in survival yield compared with conventional ESI-MS for leucine enkephalin and bradykinin of ~15% and 11%, respectively. The survival yields for liquid LEMS analyses were comparable to or better than ESI-MS for benzylpyridinium salts and large biomolecules.

Keywords: Femtosecond vaporization, Electrospray ionization, Ambient mass spectrometry, Internal energy deposition

Received: 7 February 2014/Revised: 2 May 2014/Accepted: 16 May 2014/Published online: 11 July 2014

Introduction

The "soft" ionization methods, including electrospray ionization (ESI) [1, 2] and matrix-assisted laser desorption/ionization (MALDI) [3–5], enable the detection of intact macromolecular ions with minimal fragmentation. By comparison, electron impact ionization creates a distribution of internal energies, E_{int}, for a given molecule with a higher average because of the typical ~70 eV electron beam [6]. The internal energy of the ions controls the extent of fragmentation in the obtained mass spectrum. Measurements of the internal energy distribution deposited by a mass spectral method are important for developing improved methods. The survival yield (SY) method is a common approach for determining the internal energy of a mass spectral technique [7]. This method assumes that all ions with an internal energy below the critical energy, E_o, do not dissociate whereas all ions with an internal energy above the threshold do so. In theory, only the molecular ion is observed when $E_{int}<E_o$ and only fragment ions are observed when $E_{int}>E_o$. The survival yield measures the fraction of ions with an internal energy below the critical energy and can be calculated using Equation (1),

$$SY = \frac{I(M^+)}{\left[I(M^+) + \sum I(F^+)\right]} = \int_0^{E_o} P(E)dE \qquad (1)$$

where $I(M^+)$ and $I(F^+)$ are the intensity of the molecular and fragment ions observed in the mass spectra, respectively. The internal energy distribution, $P(E)$, can be determined by

Electronic supplementary material The online version of this article (doi:10.1007/s13361-014-0936-6) contains supplementary material, which is available to authorized users.

Correspondence to: Robert J. Levis; *e-mail:* rjlevis@temple.edu

taking the derivative of the survival yield as a function of energy using a set of ions having the same internal energy distribution but with different critical energies. The experimental internal energy distributions are collective values resulting from the various energetic states of the ionized analyte that evolve from the beginning of the analysis to the mass spectral detection. A set of ions for which the critical energy values are well-characterized and vary over a suitable range, called "thermometer" molecules, are used to determine the internal energy [7, 8].

The most common thermometer ions used are a set of substituted benzylpyridinium salts because of the relatively simple fragmentation pattern resulting from the loss of neutral pyridine leaving the benzyl cation for mass analysis, which is shown in Scheme 1. These molecules have similar masses, structures, and degrees of freedom, leading to well-characterized internal energy distributions. Benzylpyridinium ions have been extensively used to determine the "softness" of a given mass spectral technique and to determine how various parameters affect the internal energy deposition for fast atom bombardment (FAB) [9], secondary ion mass spectrometry (SIMS) [10, 11], MALDI [12–14], atmospheric pressure MALDI (AP-MALDI) [12, 15], ESI [8, 16–20], desorption electrospray ionization (DESI) [21, 22], surface-assisted laser desorption/ionization (SALDI) [23], silicon nanoparticle-assisted laser desorption/ionization (SPALDI) [24], direct analysis in real time (DART) [25], surface acoustic wave nebulization (SAWN) [26], and laser ablation electrospray ionization (LAESI) [27].

A recently developed ambient mass spectrometric technique, laser electrospray mass spectrometry (LEMS), employs an intense 800 nm femtosecond laser to induce nonresonant vaporization of samples from a surface, followed by capture and postionization by an electrospray ionization source. No sample preparation is required in the LEMS method because of nonresonant, multiphoton vaporization from the surface by intense femtosecond laser pulses (10^{13} W/cm^2). This method has been used for mass spectral analysis of small biomolecules [28, 29], proteins [30–32], lipids [33], explosives [34–36], smokeless powders [37], narcotics [38], pharmaceuticals [38], and tissues [39, 40]. Although the internal energy distribution after femtosecond laser vaporization has not been measured, previous studies have shown differences in the amount of fragmentation when comparing mass spectra obtained with LEMS and conventional electrospray mass spectrometry. LEMS analyses of dried irinotecan HCl [29] and dried tetrabutylammonium iodide [41] have resulted in more fragmentation compared with conventional electrospray analysis. On the other hand, the folded state of lysozyme was better preserved using liquid LEMS analyses than conventional ESI-MS when subjected to high collision induced dissociation (CID) energies [31].

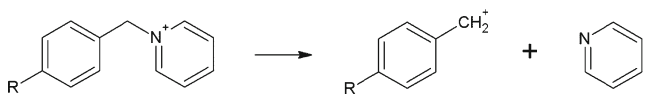

Scheme 1. Dissociation pattern of p-substituted benzylpyridinium ions into the benzylium cation and neutral pyridine

Here, we use the survival yield method to characterize the internal energy deposited during LEMS analyses of dried and liquid samples and make comparisons to conventional electrospray-mass spectrometry analyses. Para-substituted benzylpyridinium ions are used to investigate the internal energy deposition of small molecules and the peptides leucine enkephalin and bradykinin are used to gain insight on the energy deposited into larger molecules.

Experimental

Synthesis and Preparation of p-Benzylpyridinium Salts

All starting materials for the synthesis of p-benzylpyridinium (BzPy) salts were used as received from Sigma Aldrich (St. Louis, MO, USA). The benzylpyridinium salts were synthesized as described [24, 26], with the reactions performed under an argon atmosphere. The methoxy- (p-MeO), methyl- (p-Me), cyano- (p-CN), and nitro- (p-NO_2) p-substituted benzylpyridinium salts were synthesized by mixing the respective p-benzyl chloride with an excess of anhydrous pyridine in dry acetonitrile at room temperature overnight. The p-chlorobenzylpyridinium (p-Cl) salt was prepared by heating a solution of the benzyl halide and excess pyridine in acetonitrile to 80°C for 3 h. After completion of the reaction, the salts were precipitated with diethyl ether that was subsequently removed by evaporation, diluted with 1:1 (v:v) acetonitrile/water, frozen with liquid nitrogen, and lyophilized. The purified salts were diluted to 2 mM stock solutions using HPLC grade water and stored in the refrigerator prior to analysis. After initial experimentation and for verification of purity, the benzylpyridinium salts were concentrated in DMSO, purified using an Xterra Prep C18 (10×150 mm, 5 µm particle) column (Waters Corporation, Milford, MA, USA) on an Agilent 1100 series HPLC (Agilent Technologies, Inc., Santa Clara, CA, USA), lyophilized, and diluted in methanol/water using HPLC grade methanol (Fisher Scientific, Fair Lawn, NJ, USA).

The stock BzPy solutions were diluted to 1 mM in 1:1 (v:v) methanol/water and 20 µM in 1:1 methanol/water with 1% acetic acid for LEMS analyses of dried samples and conventional electrospray analyses, respectively. Solutions for LEMS analyses from liquid samples were prepared as follows: 500 µM in 1:1 methanol/water for p-MeO, p-Me, and p-Cl BzPy ions; 1.71 mM in water for p-CN BzPy; and 1 mM in 1:1 methanol/water for p-NO_2 BzPy.

Other Materials and Sample Preparation

All solid samples were used without further purification and were diluted to obtain stock solutions of 1 mM. The peptide

samples of leucine enkephalin (Tyr-Gly-Gly-Phe-Leu) acetate salt hydrate (Sigma Aldrich) and bradykinin (Arg-Pro-Pro-Gly-Phe-Ser-Pro-Phe-Arg) (AnaSpec, Fremont, CA, USA) were diluted in water, whereas the pharmaceutical irinotecan HCl (Sigma Aldrich) was diluted in 1:1 (v:v) methanol/water. For individual conventional electrospray analyses, the peptides and irinotecan HCl were diluted in 1:1 methanol/water with 1% acetic acid to obtain final concentrations of 25 μM and 20 uM, respectively. For LEMS analyses of the peptides as dried and liquid samples, the solutions were diluted to 500 μM in 1:1 methanol/water. The stock solution was used in LEMS analysis of dried irinotecan HCl.

Dried samples for LEMS analysis were prepared by spotting 15 μL aliquots on glass microscope slides (Fisher Scientific) that were cut to 7×7 mm, with each solution spotted on multiple sample slides. After allowing the sample slides to dry, the procedure was repeated once for irinotecan HCl and twice for the benzylpyridinium salts and the peptides, resulting in 30 and 45 μL of each solution deposited onto multiple sample slides, respectively. Samples for leucine enkephalin and irinotecan HCl were also spotted on 7×7 mm stainless steel sample slides for comparison with vaporization from the glass slides. To perform a LEMS measurement on a liquid sample, 10 μL was spotted on a 2.2×3.8 cm stainless steel slide and analyzed, with at least seven such samples prepared for every analyte. The sample slides were placed into the LEMS source chamber on a metal plate attached to a three-dimensional translational stage, which allowed raster scanning in order for new sample to be analyzed with every laser pulse. For temperature-controlled experiments, the translation stage was cooled using a Neslab RTE-100 refrigerated bath circulator (Neslab Instruments, Inc., Newington, NH, USA) and a custom brass plate.

Laser Electrospray Mass Spectrometry

The instrumentation for laser vaporization, electrospray postionization, and mass spectral detection has been previously described in detail [28, 30, 31, 33–35, 38–41]. A Ti:sapphire oscillator (KM Laboratories, Inc., Boulder, CO, USA) seeded a regenerative amplifier (Coherent, Inc., Santa Clara, CA, USA) to create 70 fs pulses centered at 800 nm. The laser pulse, which was focused to a spot size of ~300 μm in diameter using a 16.9 cm focal length lens with an incident angle of 45° with respect to the sample, was operated at 10 Hz to enable analysis of fresh sample and to synchronize with the hexapole operating in the trapping mode [28, 40]. The power of the laser was attenuated using a quarter-wave plate and a polarizing beam-splitting cube (CVI Laser Optics, Albuquerque, NM, USA) to a pulse energy of 1.3 mJ for the majority of the experiments, resulting in an intensity of ~2.6×10^{13} W/cm^2 at the area sampled. For laser energy studies, the pulse energy was varied from 0.7 to 2.1 mJ, corresponding to an intensity range of ~1.4 to 4.2×10^{13} W/cm^2.

After vaporization, the sample material is captured, ionized, and transferred into a mass spectrometer by an electrospray source (Analytica of Branford, Inc., Branford, CT, USA). The acidified electrospray solvent, 1:1 (v:v) methanol/water with 1% acetic acid, was pumped through the ESI needle by a syringe pump (Harvard Apparatus, Holliston, MA, USA) at a flow rate of 3 μL/min. The electrospray plume was dried by countercurrent nitrogen gas primarily at 180°C before entering the inlet capillary. For drying gas temperature experiments, the temperature was varied from 105 to 180°C. Fragmentation of the molecules was performed by increasing the voltage between the capillary exit and the skimmer of the hexapole in the spectrometer, as seen in Figure 1. An ESI solvent background mass spectrum was acquired before vaporization of each sample set to allow background subtraction of solvent-related peaks. Each LEMS experiment resulted from the averaging of 50 laser shots, which were averaged using a digital oscilloscope (LeCroy Wavesurfer 422; LeCroy Co., Chestnut Ridge, NY, USA). At least 15 and seven separate measurements were performed for LEMS analyses of dried and liquid samples, respectively. Three mass spectra, each consisting of averaging for 5 s, were collected for conventional ESI-MS analyses.

Calculation of Survival Yields and Internal Energy Distributions

The raw mass spectral data files obtained from the digital oscilloscope were saved using a custom Labview 8.5 program (National Instruments, Austin, TX, USA) and imported into the Cutter program [42] for integration of the peaks of interest, which were confirmed by tandem MS using conventional ESI-MS on a high resolution Bruker MicrOTOF-Q II mass spectrometer (Bruker Daltonics, Billerica, MA, USA). The M^+ and M^+-pyridine features for the BzPy ions, the $M+H^+$ and $[M+2H^+]^{2+}$ features for leucine enkephalin and irinotecan HCl, and the $[M+2H^+]^{2+}$ and $[M+3H^+]^{3+}$ features for bradykinin were isolated and fragmented using CID cell voltages ranging from 5 to 50 eV. In the benzylpyridinium MS/MS studies, the in-source collision induced dissociation (ISCID) voltage was adjusted to enable significant intensity of the M^+-pyridine feature for isolation and further fragmentation. All of the fragments verified by high resolution tandem MS were used in the calculations of the survival yields, including those other than the M^+-pyridine ion for the thermometer analysis.

The method used to calculate the internal energy distributions was based on the survival yield method [7]. The SY values calculated using Equation 1 were plotted as a function of the capillary exit voltage to reveal breakdown curves. For thermometer ions, the SY values for the five BzPy ions at one capillary exit voltage (at 280 V) were plotted as a function of their respective critical energies, E_o,

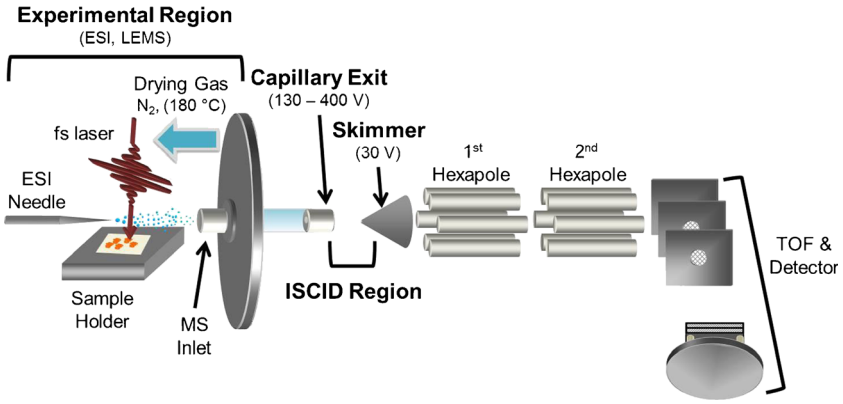

Figure 1. Schematic of the instrumental setup. The experimental region is where ESI and LEMS are peformed and the in-source collision induced dissociation (ISCID) region is where fragmentation occurs in the mass spectrometer by varying the capillary exit voltage

which were previously reported [8]. Two assumed SY values of 0% and 100% at 0 and 3.5 eV, respectively, were added to the SY curve to approximate low and high energy dissociation thresholds where complete or no fragmentation would be observed. OriginPro 9 (OriginLab Co., Northampton, MA USA) was used to fit the sigmoidal curves to the experimental data points, differentiate the sigmoidal curves for the internal energy distributions and calculate the mean internal energies ($<E_{int}>$). The sigmoidal curve was fit using a Boltzmann function, as seen in Equation (2), where E is the internal energy, E_c is the energy at the centroid of the curve, A_1 is the initial SY value, and A_2 is the final SY value.

$$SY = \frac{A_1 - A_2}{1 + e^{(E - E_c)/dE}} + A_2 \quad (2)$$

Safety Considerations

Appropriate laser eye protection was worn by all lab personnel.

Results and Discussion

Mass Spectra of Thermometer Ions Using LEMS

To characterize the energy distributions of molecules vaporized by nonresonant femtosecond laser pulses centered at 800 nm, the mass spectra of five para-substituted benzylpyridinium (BzPy) ions were measured using laser electrospray mass spectrometry (LEMS) and compared with conventional ESI-MS. LEMS measurements were collected for BzPy ions from both dried and liquid states on glass and metal substrates, respectively.

Figure 2 shows the mass spectra obtained at low and high collision energies for p-Me and p-Cl BzPy ions analyzed using conventional ESI-MS (Figure 2a and d), dried LEMS (Figure 2b and e), and liquid LEMS (Figure 2c and f). The mass spectra at low and high collision energies for the other three thermometer ions, p-MeO, p-CN, and p-NO_2 are presented in Figure S1 in Supplementary Material. The *m/z* values for all features of interest are denoted on the mass spectra with the parent molecular (M^+) and parent minus

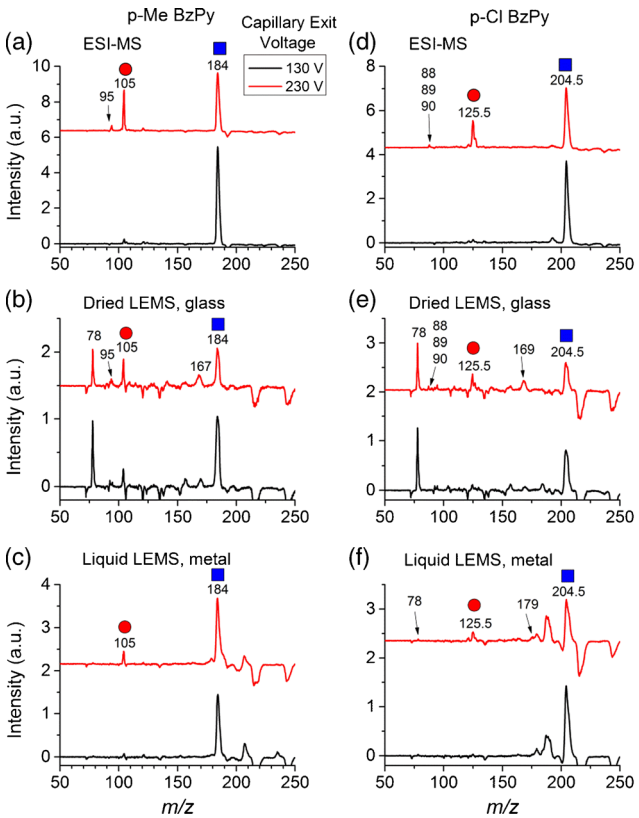

Figure 2. Mass spectra obtained for **(a)**–**(c)** p-Me and **(d)**–**(f)** p-Cl benzylpyridinium ions using **(a)** and **(d)** conventional electrospray, **(b)** and **(e)** LEMS of dried samples from glass, and **(c)** and **(f)** LEMS of liquid samples from metal. The plots show the fragmentation of the ions at low and high capillary exit voltages of 130 and 230 V as black and red lines, respectively. The M^+ and M^+-pyridine features are denoted by the blue squares and red circles, respectively

pyridine (M^+-Pyr) features highlighted as blue squares and red circles, respectively. The corresponding masses and dissociation energies of the BzPy salts are shown in Table 1. The intensities of the parent and fragment ions are related to the internal energies resulting from each of the analysis techniques. We note that peaks other than the M^+ and M^+-Pyr features were observed in the mass spectra, specifically in the LEMS analyses of dried thermometer ions. Some of these features, such as those at *m/z* 78 for all BzPy ions, were the most intense peaks in the LEMS analyses of dried thermometer ions. Fragments other than M^+-Pyr can also be seen in the conventional ESI-MS and LEMS analyses of liquid samples as well, but were less prevalent than in dried LEMS analyses. Negative features observed in the blank-subtracted mass spectra result from the vaporized analytes competing for charge and thus altering the solvent ion distribution. Positive features in the mass spectrum that are not labeled in the blank-subtracted mass spectra are solvent-related features.

To determine whether the mass spectral features other than M^+-pyridine, such as *m/z* 78, resulted from fragmentation of the BzPy ions, tandem MS was performed on the isolated M^+ and M^+-pyridine ions in a collision cell using a high resolution mass spectrometer with conventional ESI-MS. The ESI-MS/MS mass spectra are shown in Figures S2 to S6 in Supplementary Material. Most of the fragment ions detected in our ESI-MS and LEMS experiments have been observed previously [26, 43]. Table S1 in Supplementary Material lists the observed ions as well as those that were included in the survival yield calculations for the LEMS experiments. The additional fragments observed in LEMS experiments result from reaction pathways other than the simple loss of a neutral pyridine. This includes intramolecular rearrangements [43] and rearrangement to the tropylium cation [20, 44, 45].

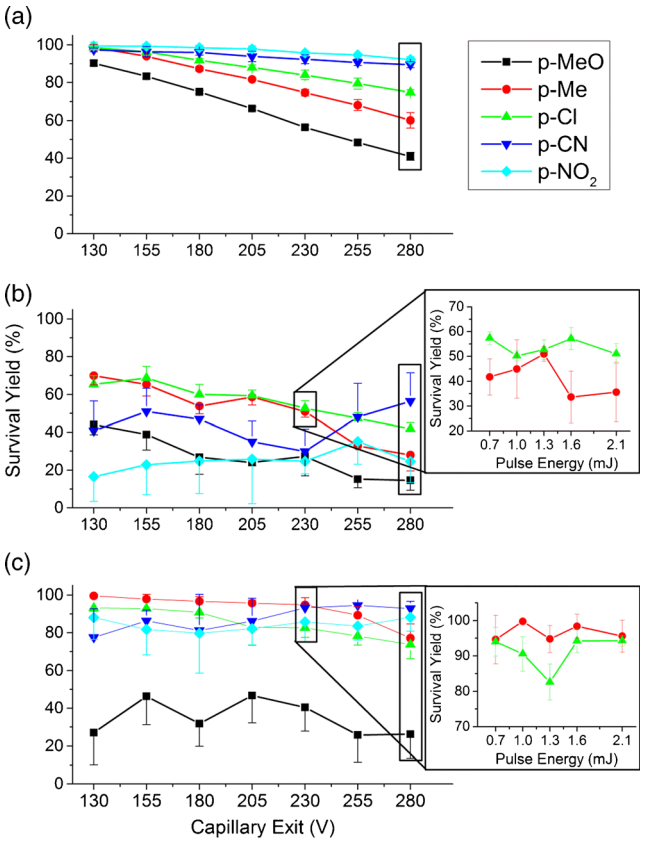

Figure 3. Breakdown curves for the p-substituted benzylpyridinium ions as a function of capillary exit voltage for **(a)** conventional ESI-MS, **(b)** LEMS of dried samples from glass, and **(c)** LEMS of liquid samples from metal. The insets in **(b)** and **(c)** show the effect of the pulse energy on survival yield at a capillary exit voltage of 230 V for p-Me and p-Cl BzPy dried and liquid samples, respectively. The box around the symbols at a capillary exit voltage of 280 V indicates the voltage chosen for the internal energy distribution calculations

Survival Yields and Internal Energy Distributions for LEMS Compared with ESI-MS

Survival yields for the five thermometer ions were calculated using Equation (1) and plotted as a function of collision energy for ESI and LEMS experiments in Figure 3. The descending order of survival yield for p-NO_2 to p-MeO BzPy in the breakdown curves for ESI-MS (Figure 3a) are in good agreement with the critical energy values, E_o. Ions with high critical energy values (p-NO_2 BzPy) do not dissociate as easily as those with low E_o values (p-MeO), resulting in less fragmentation and a larger yield of parent ions for the high E_o molecules. p-MeO had the lowest survival yield values in all experiments, in agreement with its low critical energy.

The LEMS measurements differ in several respects from the survival yield/critical energy trends observed in the ESI measurements. Although p-CN and p-NO_2 BzPy ions have the highest critical energy values, they had lower survival yields than p-Me and p-Cl in dried LEMS analyses (Figure 3b) for capillary exit voltages ranging from 130 to 230 V. At 255 and 280 V, p-CN had the highest survival yield but p-NO_2 was still lower than p-Me and p-Cl. A similar trend is noted for the analysis of liquid samples using LEMS (Figure 3c), although the overall survival yields were much higher in comparison with dried LEMS analyses. p-

Table 1. Dissociation Critical Energies and Major Mass Spectral Features Expected for the Benzylpyridinium Ions

Analyte	Eo (eV)[a]	M^+ (*m/z*)	M^+ - Pyridine (*m/z*)
p-MeO	1.51	200.3	121.2
p-Me	1.77	184.3	105.2
p-Cl	1.90	204.7	125.6
p-CN	2.10	195.2	116.1
p-NO_2	2.35	215.2	136.1

[a]Taken from Reference [8].
M^+: molecular ion, E_o: critical energy.

NO_2 BzPy had the second highest survival yield at 280 V in the LEMS analysis as a liquid sample, although it should have the highest SY. The non-intuitive increase in survival yield with increasing capillary exit voltage for p-CN and p-NO_2 resulted from the combination of the masking of low mass ions due to optimization for high mass ions and the enhanced dissociation to low mass ions at higher collision energy. The enhanced dissociation and masking effect is supported by the normalized total ion yield plots (Figure S7 in Supplementary Material), which show a decrease in the total ion yield as a function of capillary exit voltage for analyses with ESI-MS and LEMS of dried samples. Conversely, the total ion yields for most of the BzPy ions vaporized as liquid samples increased or remained unchanged, suggesting that less energy is deposited into the internal modes of the liquid sample. The shift in the ion transmittance was most apparent in the survival yields from the vaporization of dried BzPy ions, presumably because the interaction with the laser pulses resulted in a greater degree of fragmentation. We propose that dissociation of the benzyl cation fragments into a mass range not detected by our mass spectrometer plays a major role in the survival yield calculation.

To calculate the internal energy distributions [8], the survival yields obtained at a capillary exit of 280 V were plotted as a function of critical energy, E_o, in Figure 4a. This exit voltage displayed the greatest spread in the internal energy distribution for ESI-MS. The fit of the sigmoidal curve using the Boltzmann function (Equation (2)) had R^2 values of 0.992, 0.997, and 0.951 for conventional ESI-MS, dried LEMS, and liquid LEMS analyses, respectively. Note that the survival yield for the p-NO_2 benzylpyridinium ion was not included in the sigmoidal fit for dried LEMS analyses as this data point was clearly invalid and resulted in a sigmoidal curve that did not fit the majority of the points, as shown in Figure S8 in Supplementary Material. This particular ion was excluded from the data set because a large solvent feature obscured the parent molecular ion of p-NO_2 benzylpyridinium. The derivative of the sigmoidal curve provides the internal energy distribution, *P(E)*, which appears in Figure 4b for the three experimental techniques. The mean of the internal energy distributions, $<E_{int}>$ for conventional ESI-MS, dried LEMS, and liquid LEMS analyses were 1.62±0.06, 2.0±0.5, and 1.6±0.3 eV, respectively, with full width at half maximum (FWHM) of 0.96, 1.04, and 0.50 eV, respectively. Each $<E_{int}>$ uncertainty was estimated by multiplying the $< E_{int} >$ value by the average of the relative standard deviations of the survival yield values from Figure 4. The data suggest that LEMS of dried samples deposits more energy into the system than conventional electrospray with a 24.7% increase in $<E_{int}>$. However, analyses with liquid LEMS resulted in a comparable $<E_{int}>$ to conventional ESI-MS. We note that if the mass spectrometer had been tuned to have a low mass cutoff of *m/z* 100, M^+-pyridine would have been the only major fragment included in the SY calculations, resulting in similar

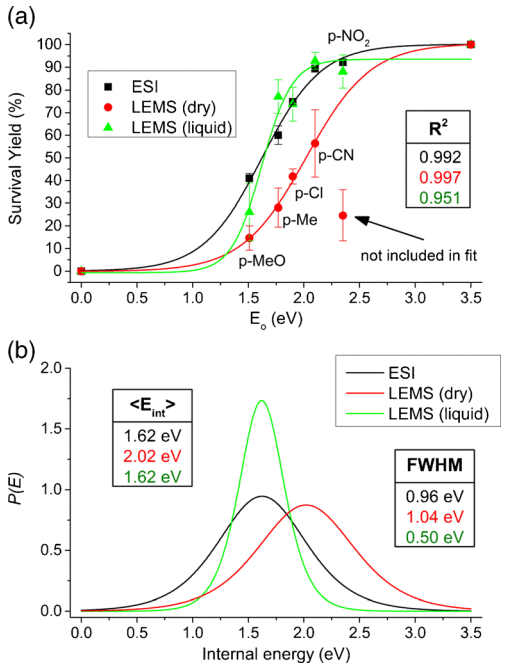

Figure 4. Internal energy deposition of LEMS compared with conventional ESI-MS. **(a)** Survival yield values were plotted as a function of critical energy, E_o, at a capillary exit of 280 V. The derivatives of the sigmoidal curves produced the **(b)** internal energy distributions [*P*(*E*)]. The sigmoidal fit R^2, mean internal energy, $<E_{int}>$, and full width at half maximum (FWHM) internal energy values for each technique are shown as tables in the figure. Note that the sigmoidal fit for dried LEMS analyses (red) does not include the survival yield for the p-NO_2 benzylpyridinium ion

internal energy distributions for all three techniques (Figure S9 in Supplementary Material). All of the fragments observed in the tandem MS measurements were included in the SY calculations [43].

Investigating the High Internal Energy Deposition in Dried Samples with LEMS

That LEMS analyses of dried BzPy ions led to more fragmentation than in conventional ESI-MS is not unanticipated as certain small molecules have been previously observed to have additional fragmentation in the case of laser vaporization [29, 41]. Yet, it was surprising that dried and liquid benzylpyridinium LEMS analyses resulted in completely different internal energy distributions. Therefore, further experiments were conducted to elucidate a potential mechanism of high internal energy deposition with dried samples, including investigations concerning the drying gas temperature, the substrate material, the sample holder temperature, the sample drying process, and the interaction with the laser. The results of these experiments for p-Me and p-Cl BzPy are shown and discussed in detail in Figure S10 in Supplementary Material. Briefly, the

results suggested that the drying gas temperature, the substrate material, the sample holder temperature, and the sample drying process did not significantly contribute to the excess fragmentation observed in LEMS analyses of dried benzylpyridinium salts.

Interaction with highly intense femtosecond laser pulses typically induces non-thermal, nonresonant, and universal vaporization of molecules [46]. However, if a molecule has a low order multiphoton resonance, fragmentation may occur, particularly in the ionic state [47, 48]. UV-visible spectra were measured for the benzylpyridinium ions to determine if the molecules had a resonance with 800 nm light (Figure S11 in Supplementary Material). There was no absorption at 800 nm but there was an absorption centered at 400 nm for all of the benzylpyridinium ions except for p-CN BzPy. Although the UV-Vis measurement is a one-photon process, two-photon absorption is possible since the molecules lack a center of symmetry. UV-visible spectra were measured for the two previously reported LEMS investigations of dried samples that resulted in a greater amount of fragmentation than with conventional ESI-MS [29, 41]. Tetrabutylammonium iodide, which loses one of its butyl groups because of femtosecond laser vaporization [41], had a broad absorption centered at ~360 nm that extends above 400 nm, as seen in Figure S12 in Supplementary Material. Irinotecan HCl, which is studied in detail in the next section, also had an absorption centered at ~355 nm that extends to 400 nm (Figure S13c in Supplementary Material). Two-photon excitation was possible for tetrabutylammonium iodide and irinotecan HCl given the broad bandwidth of the 70 femtosecond pulse and the broad absorption features measured for the molecules. Two-photon excitation occurred from the fringes of the 800 nm laser pulse for tetrabutylammonium iodide and irinotecan HCl and the lower intensities led to smaller absorption cross-sections and reduced fragment ratios. In comparison, benzylpyridinium ions have two-photon resonances at the most intense wavelength of the laser pulses, leading to excessive fragmentation in dried LEMS analyses.

If a two-photon resonance was the cause of excessive fragmentation in the dried LEMS analyses, the question then arises concerning *why the fragmentation pattern was different for the liquid LEMS analyses?* The data suggest that there are different mechanisms for femtosecond vaporization of dried samples and liquid samples. Femtosecond vaporization of the dried BzPy samples resulted in the majority of the energy going into the analyte's internal energy, inducing a great extent of fragmentation. However, in the analysis of liquid samples, the energy was not solely absorbed by the analytes but also by the liquid, yielding less fragmentation with survival yields similar to those obtained with conventional electrospray mass spectrometry. The liquid may also have protected the analyte from energetic collisions with the hot drying gas, therefore decreasing the internal energy. Conversely, the dried samples were vaporized directly into the drying gas prior to capture by the electrospray solvent.

Analysis of Larger Biomolecules

LEMS and ESI measurements were performed on larger biomolecules to investigate the internal energy distribution for systems with many more degrees of freedom. In general, the available degrees of freedom for the molecule and collision gas affect the resulting internal energy distribution of the molecule [8, 49], with larger molecules having lower average internal energies for equivalent collision energy. The peptides leucine enkephalin (leu-enk) (556.6 Da) and bradykinin (BK) (1060.2 Da) were analyzed from dried and liquid conditions to determine the effect of molecular weight on nonresonant, femtosecond vaporization. The possibility of two-photon resonances is reduced as these peptides do not have UV-visible absorptions around 400 nm, as seen in Figure S13b and f in Supplementary Material. Leucine enkephalin has been extensively used to study the internal energy deposition using ESI-MS [8, 18, 19, 49, 50]. Dried irinotecan HCl (623.1 Da) was also analyzed with LEMS to examine the fragmentation as a function of molecular size when two-photon resonant fragmentation is prevalent as this molecule has an absorbance extending to 400 nm.

Analysis of Leucine Enkephalin

The conventional electrospray and LEMS mass spectra obtained for leucine enkephalin, irinotecan HCl, and bradykinin are presented in Figure 5a–c, d–e, and f–h, respectively, at low and high capillary exit voltages. The corresponding breakdown curves (survival yield as a function of capillary exit voltage) are plotted in Figure 6a–c, respectively, for the three biomolecules. The high resolution ESI-MS/MS mass spectra of the isolated parent peaks and the fragmentation features included in the SY calculations are presented in Figures S14 to S16 and Table S2 in Supplementary Material, respectively.

The fragmentation pattern from the LEMS analysis of dried leucine enkephalin (Figure 5b) matched the fragments observed from conventional ESI-MS (Figure 5a), though the LEMS analysis had a slightly higher yield of fragments. The survival yield for dried LEMS analysis decreased as a function of increasing ISCID energy, as seen in the breakdown curves in Figure 6a in accord with expectations. The extra fragmentation resulted in average decreases in survival yield of ~15% (excluding the data point at 130 V) and ~9% for dried LEMS analysis from glass and metal, respectively, in comparison with conventional ESI-MS. Leucine enkephalin does not have a two-photon resonance but does have an absorption at 274 nm (Figure S13a in Supplementary Material) leading to a possible three-photon resonance occurring around 267 nm. Vaporization of leucine enkephalin from metal or glass substrates resulted in little to no difference in the fragmentation pattern or survival yield. An increase in the pulse energy from 0.7 to 2.1 mJ resulted in a ~15% decrease in the survival yield for dried leucine enkephalin analysis from both glass and metal substrates, as

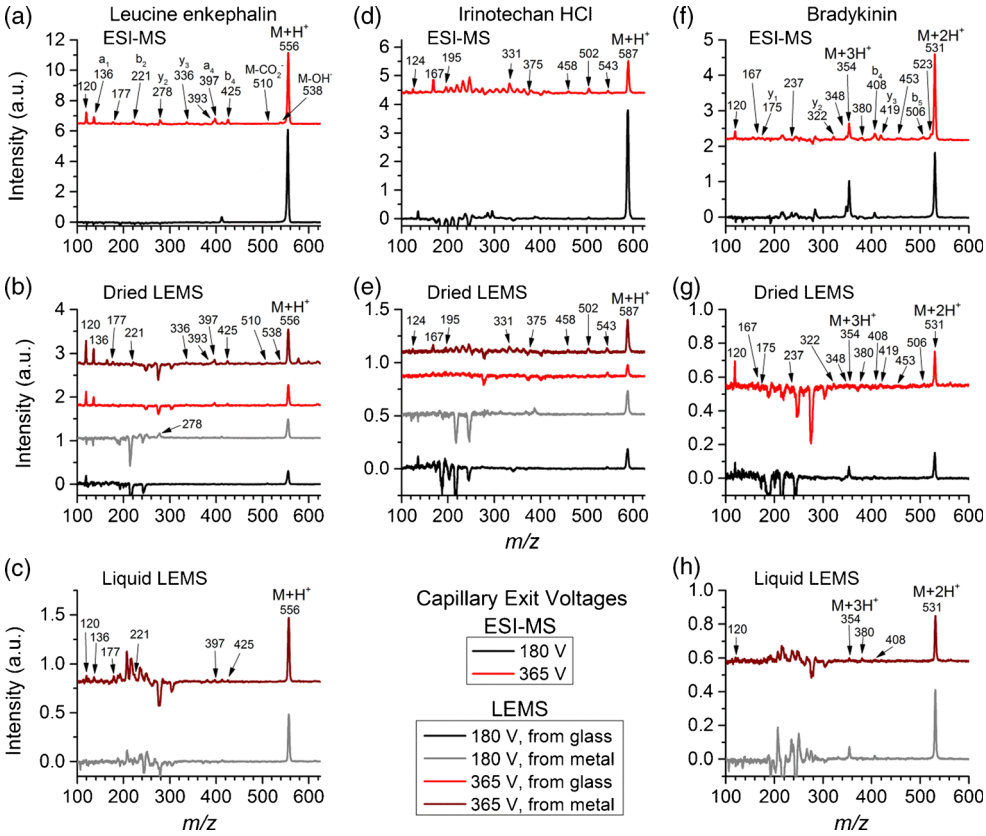

Figure 5. Mass spectra obtained for **(a)–(c)** leucine enkephalin, **(d)–(e)** irinotecan HCl, and **(f)–(h)** bradykinin using **(a)**, **(d)**, and **(f)** conventional electrospray, **(b)**, **(e)**, and **(g)** LEMS of dried samples, and **(c)** and **(h)** LEMS of liquid samples from metal. The plots show the fragmentation of the biomolecules at low and high capillary exit voltages of 180 and 365 V as black/gray and red/dark red lines, respectively

seen in the inset in Figure 6a. LEMS measurements for liquid leucine enkephalin led to less fragmentation and an increase in the survival yield, showing a similar outcome to benzylpyridinium analysis. Most of the major features in the mass spectra for the LEMS liquid analysis (Figure 5c) were solvent-related features from *m/z* 200 to 300. The survival yield as a function of ISCID potential was essentially unchanged as a function of collision energy for liquid leucine enkephalin analysis. At lower ISCID biases, analysis of liquid leucine enkephalin with LEMS resulted in an 8% lower survival yield compared with ESI. However, after the capillary exit voltage of 230 V, the survival yield decreased for ESI-MS but not for liquid LEMS analyses, resulting in 14% less fragmentation for liquid LEMS. Increasing the laser pulse energy did not result in a decrease of survival yield for liquid LEMS analysis that was observed in the dried LEMS analysis. The leucine enkephalin measurements are consistent with the BzPy studies and further support the idea that resonances lead to dissociation.

Analysis of Irinotecan HCl

Mass analysis of irinotecan HCl was revisited since it previously had been shown to fragment more with LEMS than with ESI-MS [29]. The mass spectra are shown in Figure 5d–e for conventional ESI-MS and dried LEMS, respectively. Like the leucine enkephalin study, the fragments observed during LEMS analyses correspond well to those from conventional ESI. Vaporization of irinotecan HCl from glass resulted in lower survival yields in comparison with those measured using a metal substrate by an average of ~34%. Vaporization of dried p-Me BzPy (Figure S10b) from glass also resulted in lower survival yields than from metal, but this was not observed for p-Cl BzPy (Figure S10e). Further experiments are needed to explain this phenomenon. At lower capillary exit voltages (up to 230 V), LEMS analyses from a metal substrate resulted in a 9% decrease in survival yield, whereas vaporization from glass yielded a 31% decrease in comparison with ESI. This is consistent with the excess fragmentation in previous LEMS experiments of irinotecan HCl. But the survival yields for the LEMS analyses did not decrease until a capillary exit voltage of 330 V, causing LEMS analyses to display greater survival yields than ESI-MS at higher collision energies. This is analogous to the LEMS measurements of dried benzylpyridinium ions where the survival yields were consistent or increased as the CID energy increased. The increase in survival yield as a function of

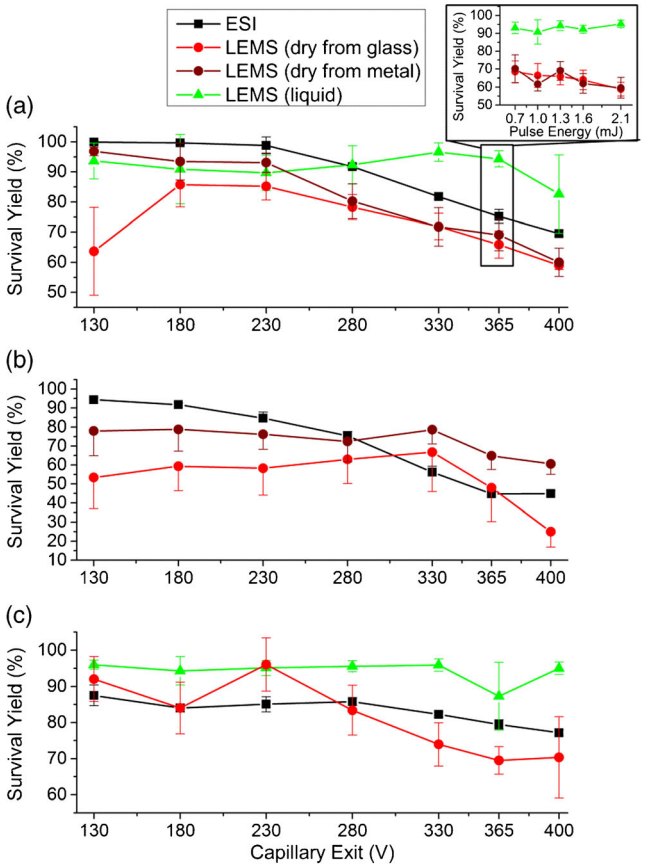

Figure 6. Breakdown curves as a function of capillary exit voltage for the biomolecules **(a)** leucine enkephalin, **(b)** irinotecan HCl, and **(c)** bradykinin using conventional ESI-MS (black ■), LEMS of dried samples from glass (red •) or metal (dark red •), and LEMS of liquid samples from metal (green ▲). The inset in **(a)** shows the effect of the pulse energy on survival yields at a capillary exit voltage of 365 V for leucine enkephalin dried and liquid samples

capillary exit voltage is again attributed to the preferred ion transmittance of higher mass ions as the ISCID potential increases, causing much of the fragment intensity to be unobserved and thereby raising the survival yield.

Analysis of Bradykinin

The mass spectra for bradykinin are presented in Figure 5f–h, and the ion intensities are shown up to *m/z* 625 to highlight the lower mass $[M+2H^+]^{2+}$ and $[M+3H^+]^{3+}$ features. The full mass spectra are shown in Figure S17 in Supplementary Material. The trends for bradykinin are similar to leucine enkephalin; the fragmentation features for electrospray and LEMS of dried samples are similar, whereas LEMS analysis of liquid samples displayed fewer fragments and solvent-related features from *m/z* 200 to 300. One major difference among the mass spectra concerns the intensity ratio of the $[M+2H^+]^{2+}$ and $[M+3H^+]^{3+}$ features, where ESI had the highest $[M+3H^+]^{3+}/[M+2H^+]^{2+}$ ratio throughout all the collision energies, as seen in Figure S18 in Supplementary Material. The LEMS analysis of dried bradykinin had the second highest ratio at lower collision energies but fell below the LEMS liquid analysis after an ISCID potential of 230 V as vaporization of bradykinin from aqueous solution resulted in no change in the $[M+3H^+]^{3+}/[M+2H^+]^{2+}$ ratio. There was also no change in the survival yield as a function of collision voltage for liquid LEMS analysis, as shown in the breakdown curves (Figure 6c), as the SY remained around 95% with a 13% average increase compared with conventional electrospray. The breakdown curves show that the vaporization of dried bradykinin led to initial internal energies that were consistent with ESI-MS until higher collision energies, where an average decrease in survival yield of about 11% occurred for dried LEMS. This is consistent with the hypothesis that the mechanism of vaporization for dried samples and liquid samples is different. The dried LEMS SY data point at the capillary exit of 230 V was uncharacteristically high in comparison with the rest of the data and may be an outlier. In parallel with the leucine enkephalin experiment, bradykinin may have a three-photon resonance as it has an absorption centered at 256 nm (Figure S13c in Supplementary Material). The measurements reaffirm the capability of femtosecond vaporization to preserve the conformation of a protein from its condensed phase as was observed previously for aqueous lysozyme [31].

Conclusions

LEMS measurements with 800 nm femtosecond laser pulses for dried and liquid samples resulted in more internal energy deposited into dried samples than solution-phase samples. Analysis of liquid samples resulted in less fragmentation, presumably through the solvent mitigating the amount of internal energy transferred to the molecules. The decrease in fragmentation may also be due to solvent clusters protecting the molecules from the hot drying gas in the case of LEMS of liquid analytes. A two-photon resonance resulted in a substantial increase in fragmentation in the analysis of dried benzylpyridinium ions, tetrabutylammonium iodide, and irinotecan HCl. The internal energy distributions for dried samples were dependent on the molecular weight, with smaller molecules subject to more fragmentation and lower survival yields. Femtosecond vaporization of molecules from the solution-phase led to internal energies that are comparable to those obtained with conventional electrospray, regardless of a multiphoton resonance. To obtain the "softest" analysis, liquid samples can be vaporized with 800 nm femtosecond laser pulses at any pulse energy, whereas dried samples should be desorbed with the lowest possible pulse energies, particularly if the molecule has a multi-photon resonance with the laser light.

Acknowledgments

The authors acknowledge support for this work by the Office of Naval Research (N00014-10-0293) and the National Science Foundation (CHE 0957694).

References

1. Yamashita, M., Fenn, J.B.: Electrospray ion source. Another variation on the free-jet theme. J. Phys. Chem **88**, 4451–4459 (1984)
2. Whitehouse, C.M., Dreyer, R.N., Yamashita, M., Fenn, J.B.: Electrospray interface for liquid chromatographs and mass spectrometers. Anal. Chem. **57**, 675–679 (1985)
3. Tanaka, K., Waki, H., Ido, Y., Akita, S., Yoshida, Y., Yoshida, T., Matsuo, T.: Protein and polymer analyses up to m/z 100 000 by laser ionization time-of-flight mass spectrometry. Rapid Commun. Mass Spectrom. **2**, 151–153 (1988)
4. Karas, M., Bachmann, D., Bahr, U., Hillenkamp, F.: Matrix-assisted ultraviolet laser desorption of non-volatile compounds. Int. J. Mass Spectrom. **78**, 53–68 (1987)
5. Karas, M., Hillenkamp, F.: Laser desorption ionization of proteins with molecular masses exceeding 10,000 daltons. Anal. Chem. **60**, 2299–2301 (1988)
6. Vékey, K.: Internal energy effects in mass spectrometry. J. Mass Spectrom. **31**, 445–463 (1996)
7. Kenttämaa, H.I., Cooks, R.G.: Internal energy distributions acquired through collisional activation at low and high energies. Int. J. Mass Spectrom. Ion Processes **64**, 79–83 (1985)
8. Gabelica, V., Pauw, E.D.: Internal energy and fragmentation of ions produced in electrospray sources. Mass Spectrom. Rev. **24**, 566–587 (2005)
9. Williams, D.H., Naylor, S.: The internal energy distribution in fast atom bombardment/liquid secondary ion mass spectra. J. Chem. Soc., Chem. Commun. (18):1408–1409 (1987)
10. Derwa, F., De Pauw, E., Natalis, P.: New basis for a method for the estimation of secondary ion internal energy distribution in 'soft'ionization techniques. Org. Mass Spectrom. **26**, 117–118 (1991)
11. De Pauw, E., Pelzer, G., Marien, J., Natalis, P. In: Benninghoven, A. (Ed.) Ion formation from organic solids (IFOS III), pp. 103–108, Springer, New York, (1986)
12. Gabelica, V., Schulz, E., Karas, M.: Internal energy build-up in matrix-assisted laser desorption/ionization. J. Mass Spectrom. **39**, 579–593 (2004)
13. Greisch, J.F., Gabelica, V., Remacle, F., De Pauw, E.: Thermometer ions for matrix-enhanced laser desorption/ionization internal energy calibration. Rapid Commun. Mass Spectrom. **17**, 1847–1854 (2003)
14. Luo, G., Marginean, I., Vertes, A.: Internal energy of ions generated by matrix-assisted laser desorption/ionization. Anal. Chem. **74**, 6185–6190 (2002)
15. Schulz, E., Karas, M., Rosu, F., Gabelica, V.: Influence of the matrix on analyte fragmentation in atmospheric pressure MALDI. J. Am. Soc. Mass Spectrom. **17**, 1005–1013 (2006)
16. Collette, C., Drahos, L., Pauw, E.D., Vékey, K.: Comparison of the internal energy distributions of ions produced by different electrospray sources. Rapid Commun. Mass Spectrom. **12**, 1673–1678 (1998)
17. Collette, C., De Pauw, E.: Calibration of the internal energy distribution of ions produced by electrospray. Rapid Commun. Mass Spectrom. **12**, 165–170 (1998)
18. Drahos, L., Heeren, R., Collette, C., De Pauw, E., Vékey, K.: Thermal energy distribution observed in electrospray ionization. J. Mass Spectrom. **34**, 1373–1379 (1999)
19. Naban-Maillet, J., Lesage, D., Bossée, A., Gimbert, Y., Sztáray, J., Vékey, K., Tabet, J.C.: Internal energy distribution in electrospray ionization. J. Mass Spectrom **40**, 1–8 (2005)
20. Zins, E.L., Rondeau, D., Karoyan, P., Fosse, C., Rochut, S., Pepe, C.: Investigations of the fragmentation pathways of benzylpyridinium ions under ESI/MS conditions. J. Mass Spectrom. **44**, 1668–1675 (2009)
21. Nefliu, M., Smith, J.N., Venter, A., Cooks, R.G.: Internal energy distributions in desorption electrospray ionization (DESI). J. Am. Soc. Mass Spectrom. **19**, 420–427 (2008)
22. Badu-Tawiah, A., Bland, C., Campbell, D.I., Cooks, R.G.: Nonaqueous spray solvents and solubility effects in desorption electrospray ionization. J. Am. Soc. Mass Spectrom. **21**, 572–579 (2010)
23. Tang, H.-W., Ng, K.-M., Lu, W., Che, C.-M.: Ion desorption efficiency and internal energy transfer in carbon-based surface-assisted laser desorption/ionization mass spectrometry: desorption mechanism (s) and the design of SALDI substrates. Anal. Chem. **81**, 4720–4729 (2009)
24. Dagan, S., Hua, Y., Boday, D.J., Somogyi, A., Wysocki, R.J., Wysocki, V.H.: Internal energy deposition with silicon nanoparticle-assisted laser desorption/ionization (SPALDI) mass spectrometry. Int. J. Mass Spectrom **283**, 200–205 (2009)
25. Harris, G.A., Hostetler, D.M., Hampton, C.Y., Fernandez, F.M.: Comparison of the internal energy deposition of direct analysis in real time and electrospray ionization time-of-flight mass spectrometry. J. Am. Soc. Mass Spectrom. **21**, 855–863 (2010)
26. Huang, Y., Yoon, S.H., Heron, S.R., Masselon, C.D., Edgar, J.S., Turecek, F., Goodlett, D.R.: Surface acoustic wave nebulization produces ions with lower internal energy than electrospray ionization. J. Am. Soc. Mass Spectrom. **23**, 1062–1070 (2012)
27. Nemes, P., Huang, H., Vertes, A.: Internal energy deposition and ion fragmentation in atmospheric-pressure mid-infrared laser ablation electrospray ionization. Phys. Chem., Chem. Phys **14**, 2501–2507 (2012)
28. Brady, J.J., Judge, E.J., Levis, R.J.: Mass spectrometry of intact neutral macromolecules using intense non-resonant femtosecond laser vaporization with electrospray post-ionization. Rapid Commun. Mass Spectrom. **23**, 3151–3157 (2009)
29. Brady, J.J., Judge, E.J., Simon, K., Levis, R.J.: Laser electrospray mass spectrometry of adsorbed molecules at atmospheric pressure. In: Proceedings of SPIE: Imaging, Manipulation, and Analysis of Biomolecules, Cells, and Tissues VIII, San Francisco, CA, 7568, 75680R, 24 Feb 2010
30. Judge, E.J., Brady, J.J., Levis, R.J.: Mass analysis of biological macromolecules at atmospheric pressure using nonresonant femtosecond laser vaporization and electrospray ionization. Anal. Chem. **82**, 10203–10207 (2010)
31. Brady, J.J., Judge, E.J., Levis, R.J.: Nonresonant femtosecond laser vaporization of aqueous protein preserves folded structure. Proc. Natl. Acad. Sci. U. S. A. **108**, 12217–12222 (2011)
32. Perez, J.J., Flanigan, P.M., Karki, S., Levis, R.J.: Laser electrospray mass spectrometry minimizes ion suppression facilitating quantitative mass spectral response for multi-component mixtures of proteins. Anal. Chem. **85**, 6667–6673 (2013)
33. Brady, J.J., Judge, E.J., Levis, R.J.: Analysis of amphiphilic lipids and hydrophobic proteins using nonresonant femtosecond laser vaporization with electrospray post-ionization. J. Am. Soc. Mass Spectrom. **22**, 762–772 (2011)
34. Brady, J.J., Judge, E.J., Levis, R.J.: Identification of explosives and explosive formulations using laser electrospray mass spectrometry. Rapid Commun. Mass Spectrom. **24**, 1659–1664 (2010)
35. Flanigan, P.M., Brady, J.J., Judge, E.J., Levis, R.J.: The determination of inorganic improvised explosive device signatures using laser electrospray mass spectrometry detection with offline classification. Anal. Chem. **83**, 7115–7122 (2011)
36. Brady, J.J., Flanigan, P.M., Perez, J.J., Judge, E.J., Levis, R.J.: Multidimensional detection of explosives and explosive signatures via laser electrospray mass spectrometry. In: Proceedings of SPIE (presented in part): Chemical, Biological, Radiological, Nuclear, and Explosives (CBRNE) Sensing XIII, Baltimore, MD, 8358, 83580X, 1 May 2012
37. Perez, J.J., Flanigan, P.M., Brady, J.J., Levis, R.J.: Classification of smokeless powders using laser electrospray mass spectrometry and offline multivariate statistical analysis. Anal. Chem. **85**, 296–302 (2013)
38. Judge, E.J., Brady, J.J., Dalton, D., Levis, R.J.: Analysis of pharmaceutical compounds from glass, fabric, steel, and wood surfaces at atmospheric pressure using spatially resolved, nonresonant femtosecond laser vaporization electrospray mass spectrometry. Anal. Chem. **82**, 3231–3238 (2010)
39. Judge, E.J., Brady, J.J., Barbano, P.E., Levis, R.J.: Nonresonant femtosecond laser vaporization with electrospray postionization for ex vivo plant tissue typing using compressive linear classification. Anal. Chem. **83**, 2145–2151 (2011)
40. Flanigan, P.M., Radell, L.L., Brady, J.J., Levis, R.J.: Differentiation of eight phenotypes and discovery of potential biomarkers for a single plant organ class using laser electrospray mass spectrometry and multivariate statistical analysis. Anal. Chem. **84**, 6225–6232 (2012)

41. Flanigan, P.M., Perez, J.J., Karki, S., Levis, R.J.: Quantitative measurements of small molecule mixtures using laser electrospray mass spectrometry. Anal. Chem. **85**, 3629–3637 (2013)
42. Shackman, J.G., Watson, C.J., Kennedy, R.T.: High-throughput automated post-processing of separation data. J. Chromatogr. A **1040**, 273–282 (2004)
43. Barylyuk, K.V., Chingin, K., Balabin, R.M., Zenobi, R.: Fragmentation of benzylpyridinium "thermometer" ions and its effect on the accuracy of internal energy calibration. J. Am. Soc. Mass Spectrom. **21**, 172–177 (2010)
44. Katritzky, A.R., Watson, C.H., Dega-Szafran, Z., Eyler, J.R.: Collisionally-activated dissociation of *N*-alkylpyridinium cations to pyridine and alkyl cations in the gas phase. J. Am. Chem. Soc. **112**, 2471–2478 (1990)
45. Zins, E.L., Pepe, C., Rondeau, D., Rochut, S., Galland, N., Tabet, J.C.: Theoretical and experimental study of tropylium formation from substituted benzylpyridinium species. J. Mass Spectrom. **44**, 12–17 (2009)
46. Brady, J.J.: Vaporization of biological macromolecules using intense, ultrafast lasers: mechanism and application to protein conformation. Ph.D. Dissertation, Temple University, Philadelphia, PA (2011)
47. Bohinski, T., Moore Tibbetts, K., Tarazkar, M., Romanov, D.A., Matsika, S., Levis, R.J.: Measurement of an electronic resonance in ground state, gas phase acetophenone cation via strong field mass spectrometry. J. Phys. Chem. Lett. **4**, 1587–1591 (2013)
48. Trushin, S., Fuß, W., Schmid, W.: Dissociative ionization at high laser intensities: Importance of resonances and relaxation for fragmentation. J. Phys. B At. Mol. Opt. Phys. **37**, 3987–4011 (2004)
49. Pak, A., Lesage, D., Gimbert, Y., Vékey, K., Tabet, J.C.: Internal energy distribution of peptides in electrospray ionization: ESI and collision-induced dissociation spectra calculation. J. Mass Spectrom. **43**, 447–455 (2008)
50. Kuki, Á., Shemirani, G., Nagy, L., Antal, B., Zsuga, M., Kéki, S.: Estimation of activation energy from the survival yields: fragmentation study of leucine enkephalin and polyethers by tandem mass spectrometry. J. Am. Soc. Mass Spectrom. **24**, 1064–1071 (2013)